

Astrophysical S-factor of $^{14}\text{N}(p, \gamma)^{15}\text{O}^*$

A. Formicola,¹ G. Imbriani,² H. Costantini,³ C. Angulo,⁴ D. Bemmerer,⁵ R. Bonetti,⁶ C. Broggini,⁷ P. Corvisiero,³ J. Cruz,⁸ P. Descouvemont,⁹ Z. Fülöp,¹⁰ G. Gervino,¹¹ A. Guglielmetti,⁶ C. Gustavino,¹² G. Gyürky,¹⁰ A. P. Jesus,⁸ M. Junker,¹² A. Lemut,³ R. Menegazzo,⁷ P. Prati,³ V. Roca,¹³ C. Rolfs,¹ M. Romano,¹³ C. Rossi Alvarez,⁷ F. Schümann,¹ E. Somorjai,¹⁰ O. Straniero,² F. Strieder,¹ F. Terrasi,¹⁴ H. P. Trautvetter,¹ A. Vomiero,¹⁵ and S. Zavatarelli³

¹*Institut für Experimentalphysik III, Ruhr-Universität Bochum, Bochum, Germany*

²*Osservatorio Astronomico di Collurania, Teramo and INFN Napoli, Italy*

³*Università di Genova, Dipartimento di Fisica and INFN Genova, Italy*

⁴*Centre de Recherches du Cyclotron, Université catholique de Louvain, Belgium*

⁵*Institut für Atomare Physik und Fachdidaktik, Technische-Universität Berlin, Germany*

⁶*Università di Milano, Istituto di Fisica and INFN Milano, Italy*

⁷*INFN Padova, Italy*

⁸*Centro de Fisica Nuclear da Universidade de Lisboa, Lisboa, Portugal*

⁹*Physique Nucléaire Théorique and Physique Mathématique, CP229,*

Université Libre de Bruxelles, Brussels, Belgium

¹⁰*ATOMKI, Debrecen, Hungary*

¹¹*Università di Torino, Dipartimento di Fisica Sperimentale and INFN Torino, Italy*

¹²*INFN Laboratori Nazionali del Gran Sasso, Assergi, Italy*

¹³*Università di Napoli, Dipartimento di Fisica and INFN Napoli, Italy*

¹⁴*Seconda Università di Napoli, Dipartimento di Scienze Ambientali, Caserta, and INFN Napoli, Italy*

¹⁵*Università di Padova, Dipartimento di Fisica, Padova and INFN Legnaro, Italy*

(Dated: November 10, 2018)

We report on a new measurement of the $^{14}\text{N}(p, \gamma)^{15}\text{O}$ capture cross section at $E_p = 140$ to 400 keV using the 400 kV LUNA accelerator facility at the Laboratori Nazionali del Gran Sasso (LNGS). The uncertainties have been reduced with respect to previous measurements and their analysis. We have analyzed the data using the R-matrix method and we find that the ground state transition accounts for about 15% of the total S-factor. The main contribution to the S-factor is given by the transition to the 6.79 MeV state. We find a total $S(0) = 1.7 \pm 0.2$ keV b, in agreement with recent extrapolations. The result has important consequences for the solar neutrino spectrum as well as for the age of globular clusters.

PACS numbers: 24.30.-v, 24.50+g, 26.20.+f

The capture reaction $^{14}\text{N}(p, \gamma)^{15}\text{O}$ ($Q = 7297$ keV) is the slowest process in the hydrogen burning CNO cycle [1] and thus of high astrophysical interest. This reaction plays a role of setting the energy production and neutrino spectrum of the sun [2] as well as the age determination of globular clusters [3]. Below 2 MeV, several ^{15}O states contribute to the $^{14}\text{N}(p, \gamma)^{15}\text{O}$ cross section (fig. 1): a $J^\pi = 3/2^+$ subthreshold state at $E_R = -507$ keV ($E_x = 6.79$ MeV), and 3 resonant states: $J^\pi = 1/2^+$ at $E_R = 259$ keV, and $3/2^+$ at $E_R = 987$ keV and $E_R = 2187$ keV. The reaction was previously studied over a wide range of energies, i.e. $E_{cm} = E = 240$ to 3300 keV ([4] and references therein). The non resonant capture to excited states in ^{15}O led the authors of ref. [4] to an extrapolated astrophysical S-factor at zero energy of $S_{es}(0) = 1.65$ keV b. The data for the capture into the ^{15}O ground state were analyzed using the Breit-Wigner formalism and indicated an important influence of a subthreshold state at $E_R = -507$ keV, leading to

$S_{gs}(0) = 1.55 \pm 0.34$ keV b with a deduced gamma width of $\Gamma_\gamma = 6.3$ eV, thus $S_{tot}(0) = 3.20 \pm 0.54$ keV b.

A reanalysis [5] of the capture data to the ground state [4] using an R-matrix approach indicated a negligible contribution of the subthreshold state to the total S(0)-factor, mainly due to a significantly smaller Γ_γ of this state. This indication was supported by a lifetime measurement of the $E_R = -507$ keV subthreshold state via the Doppler-shift method [6] leading to $\Gamma_\gamma = 0.41^{+0.34}_{-0.13}$ eV, and a measurement via the Coulomb excitation method [7] resulted in $\Gamma_\gamma = 0.95^{+0.60}_{-0.95}$ eV. In view of the uncertainties in $S_{gs}(0)$ and thus $S_{tot}(0)$, a new measurement of the capture process into the ^{15}O ground state was highly desirable, extending possibly the low energy limit below that of previous work i.e., below $E = 240$ keV. We report on the results of such measurements using the 400 kV underground accelerator facility LUNA at Gran Sasso, Italy.

The 400 kV LUNA facility and the setup have been described elsewhere [8]. Briefly, the accelerator provided a proton current on target of up to $500 \mu\text{A}$. The absolute energy is known with an accuracy of 0.3 keV and the energy spread and the long-term energy stability were observed to be 100 eV and 5 eV/h, respectively. Near the target, the beam passed a liquid-nitrogen cooled shroud

*Supported in part by INFN, BMBF(05CL1PC1), GSI(BO-ROL), OTKA(T034259 and T042733), TARI HPRI-CT-2001-00149 and SSTC PAI(P5/07)

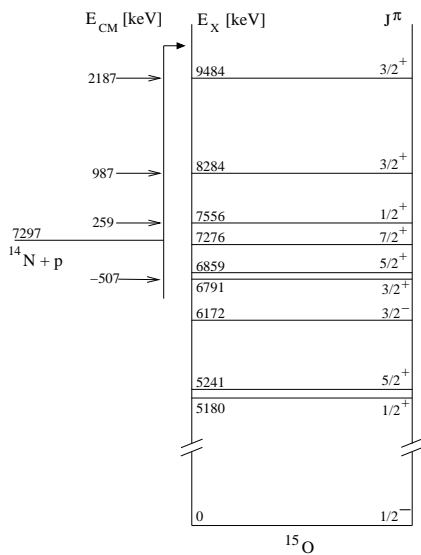


FIG. 1: Level structure of ^{15}O . Above the $^{14}\text{N}(p,\gamma)^{15}\text{O}$ threshold only relevant states are shown.

(to minimize carbon-buildup on target) and an electrically insulated collimator with a negative voltage of 300 V (to suppress the effects of secondary electrons). The water-cooled target was oriented with its normal at 55° to the beam direction. The target consisted of a TiN layer (with a typical thickness of 80 keV) reactively sputtered on a 0.2 mm thick Ta backing. The target quality was checked frequently at the $E_R = 259$ keV resonance: no significant deterioration was observed after a bombarding time of several days. Typically, a new TiN target was used after a running time of 1 week. The stoichiometry of the TiN layer was verified via Rutherford Backscattering Spectrometry using a 2.0 MeV $^4\text{He}^+$ beam, resulting in $Ti/N = 1/(1.08 \pm 0.05)$.

To deduce cross section values in the non-resonant energy region, one can use either thin targets (say, a few keV) or thick targets (say, a few 10 keV). Due to sputtering effects at low energies thin targets deteriorate significantly in a short time changing correspondingly the observed γ -ray yields. In the case of thick targets, the sputtering effect on the observed yields is negligible, as long as the thickness stays large enough, which was verified experimentally (see above). For the chosen thick targets, we made an analysis of the line shape of the primary γ -rays as described below to deduce a capture cross section.

For the measurement of excitation functions the capture γ -rays were observed with one Ge detector (126% efficiency) placed at 55° in close geometry to the target ($d = 1.53$ cm was the distance between the target and the front face of the detector). In one experiment the distance was increased up to 20.5 cm for the determination of the detector efficiency and summing effects. In another experiment, Ge detectors were placed at 0° (126 %), 90° (120 %), and 125° (108 %), relative to the beam axis ($d = 7$ cm) for the measurement of Doppler shifts, exci-

tation energies, and angular distributions. Sample spectra are shown in fig. 2 where the influence of different background sources can be observed: (a) beam induced background, which is mainly due to proton capture on ^{11}B , ^{18}O , and ^{23}Na while at $E_p = 140$ keV (b) the remaining beam induced background from ^{11}B contaminations is equal to the cosmic background.

In a similar way as described in [8], the line shape of the γ_0 -capture transition in $^{14}\text{N}(p,\gamma)^{15}\text{O}$ may be used for various purposes. Fig. 3 shows the γ_0 -ray line shape observed at $\theta_\gamma = 55^\circ$ and $E = 243$ keV, i.e. at the low-energy tail of the $E_R = 259$ keV resonance; the dispersion in the spectrum was 1 keV/channel. The line shape can be interpreted as the sum of the resonant and non resonant contributions; when convoluted with the detector resolution, the solid curve through the data points is obtained. In this way, the drop in the γ_0 -ray yield towards lower energies reflects directly the drop of the cross section. For the calculated line shape the dependence on energy of the γ_0 -efficiency and of the stopping power of protons in TiN [10] was included. The high-energy edge of the peak contains the information on the incident beam energy, hence possible C-build up on target could be corrected for; this correction was never larger than 2 keV. The method to extract the cross section from the γ_0 -ray line shape requires further investigation of the following points: (i) energy, width, branching ratios, and strength of the $E_R = 259$ keV resonance, (ii) energy calibration and efficiency of the Ge detector, (iii) summing effects in close geometry, (iv) Doppler shift, and (v) effects of angular distributions. In the same way the transition to the 6.79 MeV state was analysed. Below $E = 170$ keV the information of the data from the secondary transition was used in the analysis. For this energy region a constant $S_{6.79}$ was assumed over the target thickness. A detailed description of all these points is given elsewhere [11, 12], where a complete analysis of the data to all final states will be presented.

The resonance energy could in principle be determined from the γ_0 -energy after correction for Doppler shift and recoil. One requirement is the precise energy calibration of the Ge detector. We have used the information obtained from the experiment with the 3 Ge detectors ($\theta_\gamma = 0^\circ, 90^\circ$, and 125°). From [6] it is known, that the $E_x = 5181$ keV state in ^{15}O shows an attenuated Doppler shift and the 6172 and 6791 keV states have lifetimes resulting in nearly full Doppler shifts. Using the known energy of the resonance from the accelerator calibration together with $Q = 7296.8 \pm 0.5$ keV [13] and calibration points from radioactive sources we have performed a combined χ^2 fit of the data obtained at the three angles. It was necessary to vary also the excitation energies of the first three excited states. In addition, we varied the attenuation coefficients for the Doppler shifts. The Doppler shift data for the $E_x = 6791$ keV state are shown in Fig. 4 and all results are summarized in Table I. We confirm the results of [6] for the first excited state in ^{15}O but could not extract a lifetime for the 6791 keV

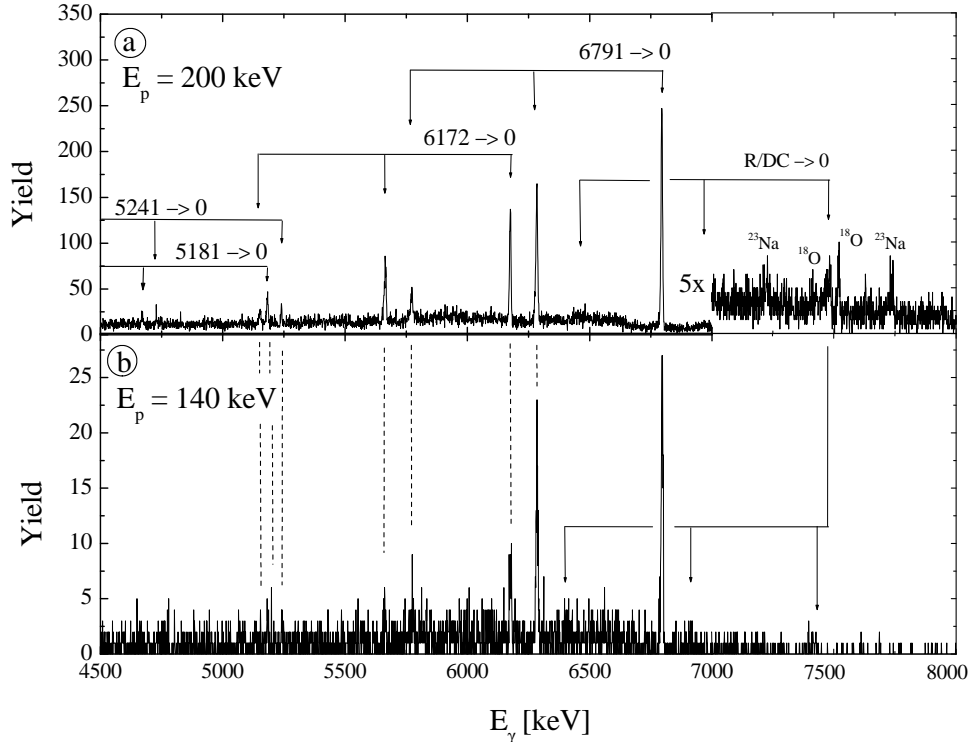


FIG. 2: γ -spectrum for $^{14}\text{N}(p, \gamma)^{15}\text{O}$ obtained (a) at $E_p = 200$ keV ($Q = 85$ C, $t = 62$ h) and (b) at $E_p = 140$ keV ($Q = 222$ C, $t = 396$ h). For case (a) beam induced background originates primarily from traces of ^{11}B , ^{18}O , and ^{23}Na in the target, while for case (b) the beam induced background was of the same order than the remaining cosmic background which is about 7 counts in the region of the peak for the ground state transition where a total of 50 counts are observed.

TABLE I: Excitation energies in ^{15}O , Doppler shift measurements and γ -branching ratios for the 259 keV resonance ($E_x = 7556$ keV).

E_x [keV]		$F(\tau)$ Doppler shift		Branching [%] ^a	
present	[9]	present ^b	[6] ^c	present	[9]
5180.51 ± 0.14	5183.0 ± 1.0	0.68 ± 0.03	0.68 ± 0.03	16.6 ± 0.2	15.8 ± 0.5
6171.86 ± 0.15	6176.3 ± 1.7	0.99 ± 0.03	0.91 ± 0.05	58.4 ± 0.3	57.5 ± 0.6
6791.23 ± 0.19	6793.1 ± 1.7	0.99 ± 0.04	0.93 ± 0.03	23.3 ± 0.3	23.2 ± 0.4
7556.23 ± 0.28	7556.5 ± 0.4			1.67 ± 0.10^d	3.5 ± 0.6^d

^afor the $E_R = 259$ keV resonance

^bTiN target

^cN implanted in Ta

^dtransition to the ground state

state due to a nearly full Doppler shift. For all the subsequent work we calibrated the γ -ray spectra using the new excitation energies given in Table I.

The detector efficiency was determined using calibrated radioactive sources and the cascade condition for the transitions to the first three excited states at the $E_R = 259$ keV resonance, as for all of them no other decay than that to the ground state was observed. This procedure was performed with the Ge detector placed at 1.53, 5.5, 10.5, and 20.5 cm distances from the target in order to determine the summing-in contribution to

the ground state transition and the summing-out for the transitions to the excited states. It turned out, that the summing-in yield was about 3.5 times higher than the actual ground state intensity at the 1.53 cm position. This 1.53 cm position was used for the entire cross section measurements. The efficiency curve was also calculated using the GEANT routine [14] and found to be in excellent agreement with observation [11]. Branching and strength values of the $E_R = 259$ keV resonance were determined with low beam current to avoid dead time effects and at far distance (20.5 cm) to minimize summing effects from

TABLE II: R-matrix parameters for capture transition to the ground state

radius a [fm]	ground state	subthreshold state		E_{res}		transition to	
	ANC C [$\text{fm}^{-1/2}$]	γ^2 [MeV]	Γ_γ [eV]	2.19 MeV Γ_γ [eV]	6 MeV Γ_γ [eV]	$E_x = 0$ MeV $S(0)$ [keV b]	$E_x = 6.79$ MeV $S(0)$ [keV b]
5	5.8	0.40	1.2	4.3	25	0.19	1.31
5.5	7.3	0.42	0.8	4.4	23	0.25	1.35
6	8.8	0.44	0.5	4.7	26	0.31	1.39
average		0.42 ± 0.02	0.8 ± 0.4	4.5 ± 0.2	23 ± 3	0.25 ± 0.06	1.35 ± 0.05

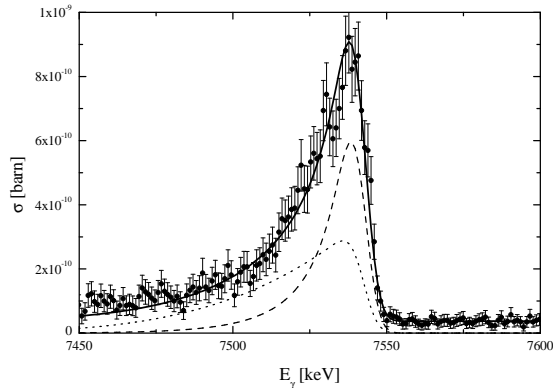


FIG. 3: Typical γ_0 -ray line shape of $^{14}\text{N}(p, \gamma)^{15}\text{O}$ obtained at $E_p = 260$ keV. The dashed line corresponds to the expected resonant part, the dotted line to the fitted non-resonant part, and the solid line is their sum including background.

cascade transitions. The branching results are given in Table I; they are in good agreement with previous work [15], except for the ground state transition. Our strength value of $\omega\gamma = 13.5 \pm 0.4$ (statistical) ± 0.8 (systematical) meV, which was determined absolutely, is also in good agreement with previous work [4, 9], $\omega\gamma = 14 \pm 1$ meV. The fitted total width of $\Gamma = 0.99 \pm 0.03$ keV is consistent with previous work ([4]: $\Gamma = 1.2 \pm 0.2$ keV).

All transitions show isotropy at the $E_R = 259$ keV, $J^\pi = 1/2^+$ resonance and no forward-backward asymmetry [11] outside the resonance. Consequently, an angle-integrated γ_0 -ray yield may be derived directly from the yield collected by the Ge detector at $\theta_\gamma = 55^\circ$. Finally, the summing due to the large solid angle of the detector and the cascade coincident events in the transition to the ground state was corrected for by studying all other capture transitions. The absolute scale of the cross section deduced from the γ -ray line shape was obtained by normalizing to the thick target yield in the 259 keV resonance [1] whose strength $\omega\gamma$ was determined absolutely (see above).

The capture data from LUNA and previous work [4] for the transition to the 6.79 MeV state are shown in figure 5: there is an excellent agreement between both data sets in the region of overlap. As shown from previous work [4, 5], the S-factor has an external non-resonant contribution

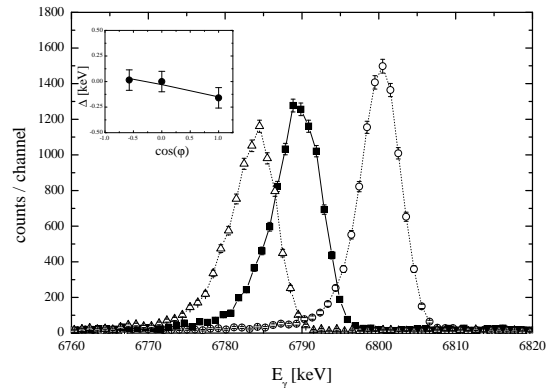


FIG. 4: Full-energy peak for the $6791 \rightarrow 0$ keV transition observed with three Ge detectors positioned at 0° (open circles), 90° (filled squares), and 125° (open triangles). The insert shows the measured energy shift relative to the expected full Doppler shift, where the solid line corresponds to the attenuation factor $F(\tau) = 0.99$.

and a contribution from the $E_R = 259$ keV resonance, where the latter contribution was derived from $\omega\gamma$ and Γ values of the present work. The R-matrix fit [5, 16] included both contributions. The resulting ANC value of $C = 5.0 \pm 0.1 \text{ fm}^{-1/2}$ agrees with indirect determinations ([17]: $C = 5.2 \pm 0.7 \text{ fm}^{-1/2}$; [18]: $C = 4.6 \pm 0.5 \text{ fm}^{-1/2}$) and leads to the fitted curve shown in figure 5. For large values of the R-matrix radius a the fit deviates from the data for energies above $E = 1$ MeV (see Fig. 5). We have adopted the results for $a = 5.5$ fm leading to the extrapolated value $S_{6.79} = 1.35 \pm 0.05$ (statistical) ± 0.08 (systematical) keV b. This value is about 20 % lower than the R-matrix fit [5] of the data from [4] alone.

The data from LUNA and previous work [4] for the ground state capture are shown in figure 6. We have corrected the previous data for summing effects, which are at most 10 % above $E = 500$ keV, except near the destructive interference structure of the $E_R = 987$ keV resonance. The data were fitted including the $3/2^+$ subthreshold state, the $1/2^+$, 259 keV, the $3/2^+$, 987 keV and the $3/2^+$, 2187 keV resonances as well as a background pole located at 6 MeV. For the subthreshold state, we used the reduced width γ^2 obtained from the fit of the data for the 6.79 MeV transition. The fit param-

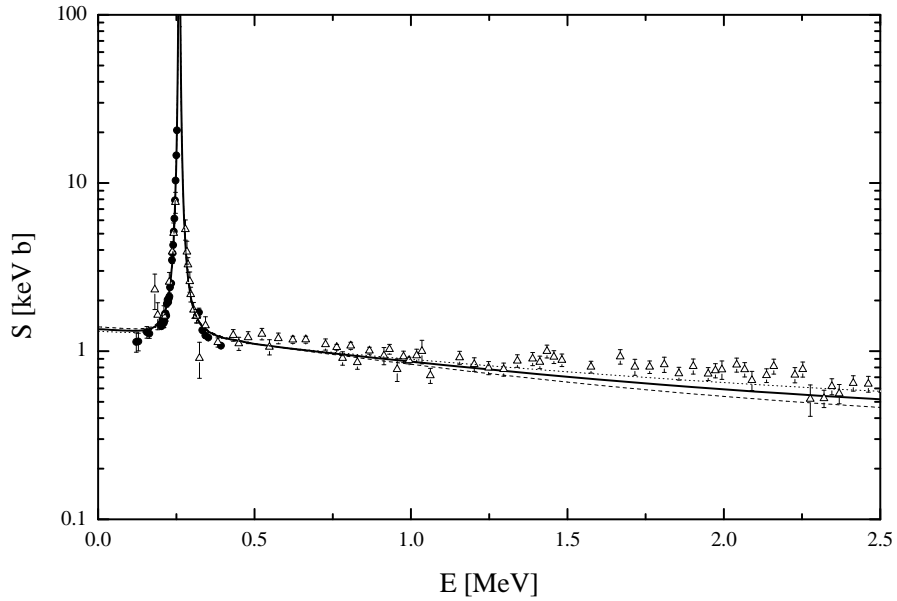


FIG. 5: Transition to the 6.79 MeV state in ^{15}O . The S-factor data from present work are represented by solid points, those of [4] by open triangles. The R-matrix fit (solid line) was obtained for $a = 5.5$ fm, the dashed line for $a = 6$ fm and the dotted line for $a = 5$ fm. The data point in the 259 keV resonance is off scale.

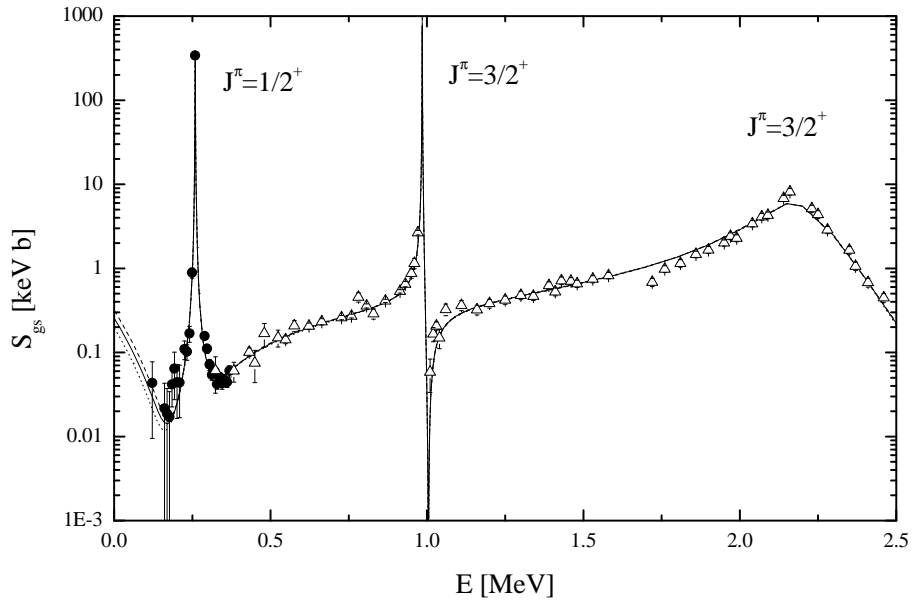


FIG. 6: Astrophysical $S(E)$ -factor curve for the ground state transition in $^{14}\text{N}(p, \gamma)^{15}\text{O}$. Filled-in data points are the results from LUNA, while the open data points are from previous work [4] correct for summing effects. The solid line corresponds to the R-matrix fit for $a = 5.5$ fm, the dashed line for $a = 6$ fm and the dotted line for $a = 5$ fm.

ters were the Γ_γ of the subthreshold state, the 987 keV and 2187 keV resonances, the Γ_p and Γ_γ of the background pole. For the external contribution we used the ANC of [17] as a starting value. The results are shown in Fig. 6 for $a = 5$ fm and $C_{gs} = 5.8$ fm $^{-1/2}$ (dotted line), $a = 5.5$ fm and $C_{gs} = 7.3$ fm $^{-1/2}$ (solid line), and $a = 6.5$ fm and $C_{gs} = 8.8$ fm $^{-1/2}$ (dashed line). The corresponding Γ_γ values for the subthreshold state and extrapolated S-factor values are listed in Table II. It can be noted that our deduced value $\Gamma_\gamma = 0.8 \pm 0.4$ eV is in good agreement with the value from a life time measurement by [6] $\Gamma_\gamma = 0.41^{+0.34}_{-0.13}$ eV as well as with $\Gamma_\gamma = 0.95^{+0.60}_{-0.95}$ eV, the value from coulomb excitation work [7]. All Γ_γ values from Table II are consistent within uncertainties with our observation of a nearly full Doppler shift for the transition of the 6.79 MeV state (see Fig. 4). The best χ^2 for the fit to the ground state transition is obtained for $a = 6$ fm ($\chi^2 = 1.27$), however the differences are small (for $a = 5$ fm, $\chi^2 = 1.35$; contributions to χ^2 near the narrow resonances have been omitted in the χ^2 values given above). The best overall agreement with all available data [4, 6, 7, 17, 18] is obtained for $a = 5.5$ fm, where our fitted ground state ANC is $C = 7.3$ fm $^{-1/2}$, that can be compared with the result of [17] which gives $C = 7.3 \pm 0.4$ fm $^{-1/2}$, after conversion to the coupling scheme used in the present work. For the total S-factor a contribution from the transition to the 6.17 MeV state of $S_{6.17}(0) = 0.06$ keV b from [5] has been added to obtain an average ($a = 5$ to 6 fm) of $S_{tot}(0) = 1.7 \pm 0.1$ (statistical) ± 0.2 (systematical) keV b, which can be compared with 1.77 ± 0.20 keV b [5] and 1.70 ± 0.22 keV b [17] from previous analyses.

In summary, the present work improves the experimen-

tal information concerning the ground state transition in $^{14}\text{N}(p, \gamma)^{15}\text{O}$. The previous data [4] corrected by summing effects discussed above are now in good agreement with the present work. The large ambiguity for the extrapolation of the ground state transition has been reduced. In the energy region between $E = 170$ to 300 keV the S(E)-factor is dominated by the 259 keV resonance. Only at energies of about 100 keV and below the contributions of the subthreshold resonance and non-resonant mechanisms should become clearly observable. Using large volume Ge detectors it is impossible to obtain additional information on $S_{gs}(E)$ at lower energies (than current work) with acceptable uncertainty due to the sizable summing correction. An improved information on $S_{tot}(E)$ can be achieved possibly using a 4π -summing crystal to observe the total S(E)-factor. Such an experiment is presently underway at the LUNA facility.

After submission of the present work several relevant publications appeared:

(i) The authors of [19] reanalyzed the data of [4] based on conclusions from their analyzing power data. This led to a different extrapolation for the transition to the 6.79 MeV state (about 10 to 20 % lower than the analysis of [5] and 11 % higher than present work) and for the transition to the 6.17 MeV state (about a factor 3 higher than [5]). However, the primary aim of the present letter was to clarify the strength of the ground state transition.

(ii) The analysis in [20, 21, 22] were partly based on the results of the present work and led to the conclusion that the solar neutrino flux from CNO cycle is reduced by a factor 2 and the age of the globular clusters is increased by about 1 billion years.

-
- [1] C.Rolfs and W.S.Rodney, *Cauldrons in the Cosmos* (University of Chicago Press, 1988).
- [2] J.N.Bahcall and M.H.Pinsonneault, *Rev.Mod.Phys.* **64**, 885 (1992).
- [3] P.A.Bergbusch and B.A.Vandenberg, *Ap.J.Suppl* **81**, 163 (1992).
- [4] U.Schröder et al., *Nucl.Phys. A* **467**, 240 (1987).
- [5] C.Angulo and P.Descouvemont, *Nucl.Phys.A.* **690**, 755 (2001).
- [6] P.F.Bertone et al., *Phys.Rev.Lett.* **87**, 152501 (2001).
- [7] K.Yamada et al., *Phys. Lett. B* **579**, 265 (2004).
- [8] A.Formicola et al., *Nucl.Instr.Meth. A* **507**, 609 (2003).
- [9] F.Ajzenberg-Selove, *Nucl. Phys. A* **523**, 1 (1991).
- [10] J.F.Ziegler and J. Biersack, *Srim-program, version 2003-20*, *srim.org* (2003).
- [11] H.Costantini (2003), Thesis, University of Genova and to be published.
- [12] A.Formicola, *Thesis* (Ruhr-Universität Bochum, 2004).
- [13] G.Audi, A.H.Wapstra, and C.Thibault, *Nucl. Phys. A* **729**, 337 (2003).
- [14] GEANT4: An Object-Oriented Toolkit for Simulation in HEP. The RD44 Collaboration, CERN/LHCC 95-70, 1995 and The Geant4 Collaboration, <http://wwwinfo.cern.ch/asd/geant4/geant4.html>.
- [15] D.F.Hebbard and G.M.Bailey, *Nuc. Phys.* **49**, 666 (1963).
- [16] A.N.Lane and R.G.Thomas, *Rev. Mod. Phys.* **36**, 257 (1958).
- [17] A.M.Mukhamedzhanov et al., *Phys. Rev. C* **67**, 065804 (2003).
- [18] P.F.Bertone et al., *Phys.Rev. C* **66**, 055804 (2002).
- [19] S.O.Nelson et al., *Phys. Rev. C* **68**, 065804 (2003).
- [20] G.Imbriani et al. (2004), astro-ph/0403071 and accepted by Astron. and Astrophy.
- [21] S.Deg'Innocenti et al. (2003), astro-ph/0312559.
- [22] J.N.Bahcall and M.H.Pinsonneault (2004), astro-ph/0402114 and accepted by Phys. Rev. Lett.